This article has been accepted for publication in a future issue of this journal, but has not been fully edited. Content may change prior to final publication. Citation information: DOI 10.1109/TIE.2017.2668982, IEEE Transactions on Industrial Electronics

Series Voltage Regulator for a Distribution Transformer to Compensate Voltage Sag/Swell

Taeyong Kang, *Student Member, IEEE*, Sewan Choi, *Senior Member, IEEE*, Ahmed S. Morsy, *Member, IEEE*, Prasad N. Enjeti, *Fellow Member, IEEE*

***Abstract* — This paper presents a series voltage regulator for a distribution transformer which addresses power quality issues in the electrical power distribution system. The proposed system is comprised of a line frequency transformer connected to a power electronic converter which is auto-connected on the secondary side. This auto-connection is facilitated by use of a high-frequency or medium frequency transformer. A simplified strategy to compensate for voltage sags and swells on the grid side, by providing continuous ac voltage regulation, is discussed. When a voltage sags or swells occur, the power electronic converter generates a compensating voltage, which is vector-added to the grid voltage in order to regulate the output voltage supplied to the load. The proposed system satisfies needs of smart distribution grids in terms of improved availability, equipment protection, and resilience. Detailed analysis is provided with experimental results in order to validate the effectiveness of the proposed system.**

***Keywords* – distribution transformer, phase-shift modulation, ride-through system, voltage sag/swell compensation**

I. Introduction

With the development of a smart grid system, highly reliable electricity supply has become an important issue [1]. A fundamental component in providing reliable electricity to the end-user is the step-down distribution transformer, as shown in Fig. 1. This distribution transformer operates at line frequency (50/60Hz) to step down from medium voltage (*MV*) to low voltage (*LV*). Even if the conventional distribution transformer is relatively inexpensive, highly efficient, and reliable, it is not guaranteed to protect loads from undesirable events such as voltage sags and swells. Voltage sags and swells have become one of the most critical power quality issues faced by many industrial consumers in power distribution systems. As the complexity of the electronics equipment used in the industrial applications grows, the customer loads are becoming more vulnerable to voltage disturbances such as sags and swells. Voltage sags/swells cost hundreds of millions of dollars every year in the United States [2-3]. The voltage sags and swells results in significant economic losses in a wide range of industries, including financial services, health care, and process manufacturing [4-7]. Consequently, it is suggested to include voltage compensation functionality in the conventional *MV/LV* step-down distribution transformer in Fig. 1.

Voltage sags and swells can be described by two essential characteristics: magnitude and duration. The survey of power quality presents that voltage sags with 40-50% of the nominal value and with duration from 2 to 30 cycles occurred in about 92% of all power system events [8]. The power acceptability curves are introduced in the bus voltage and duration time plane, as shown in Fig. 2 [9].

This work was supported in part by National Research Foundation of Korea grant funded by Korea government (No.2014R1A2A2A01003724)

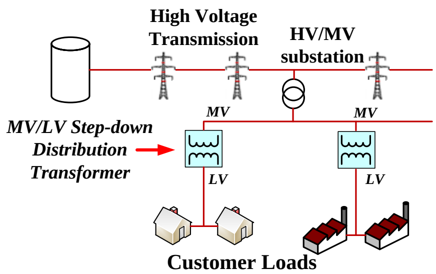

Fig. 1. Conventional Step-Down Distribution Transformer in the Distribution Grid Network.

The *ITIC* (Information Technology Industry Council) curve present acceptable voltage range between the upper locus (labeled over-voltage condition) and the lower locus (labeled under-voltage condition), which is the 'acceptable power quality' region. Hence, it is recommended to consider a deep voltage compensator for a wider range of voltage compensation over a long steady-state period.

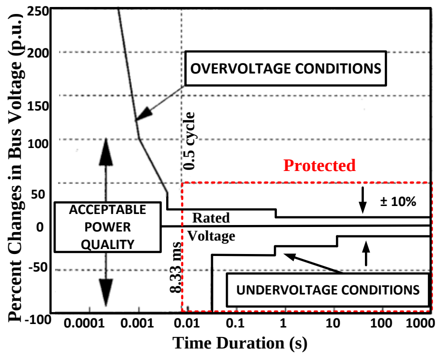

Fig. 2. (a) The *ITIC* Power Acceptability Curve [9].

In order to compensate for voltage sags and swells in the power distribution system, several approaches including on-load tap changer, dynamic sag correctors, ride-through voltage compensator, dynamic voltage restorer and hybrid distribution transformer have been developed.

The most common voltage compensator for the distribution transformer is the automatic on-load tap changers, which are integrated to most distribution transformers throughout the distribution systems. However, poor dynamics of ac voltage compensation, stepwise variation and a narrow range of output regulation are major issues to overcome in order to achieve a rapid response to voltage sags and swells [10-12].

Another possible approach to mitigate voltage disturbances which can be integrated to an existing distribution transformer is dynamic sag correctors (*DySC*) [8], [13]. The *DySC* is based on power electronics, which guarantee good dynamic characteristics by utilizing ac-ac pulse-width modulation (*PWM*) converter. Dynamic sag correctors and ride-through voltage compensators can resolve power quality problems on a customer's distribution line by providing voltage dip mitigation

This article has been accepted for publication in a future issue of this journal, but has not been fully edited. Content may change prior to final publication. Citation information: DOI 10.1109/TIE.2017.2668982, IEEE Transactions on Industrial Electronics

at a reduced cost [14-15]. In [16], a *PWM* ac-ac buck converter with auto-transformer to process partial load-power was discussed to compensate for voltage sags. However, systems introduced in [8], [13-16] have a limitation; they only compensate for voltage sag.

Additionally, an often encountered approach for sag/swell mitigation is the dynamic voltage restorer (*DVR*) which injects a voltage component in series with the load voltage [17-19]. Also a voltage compensator using direct power conversion without dc-link capacitors was proposed in [20-21]. However, these voltage compensators require an extra bulky line frequency transformer (*LFT*) and/or huge energy storage capacitors causing challenges in integrating them with the existing distribution transformer.

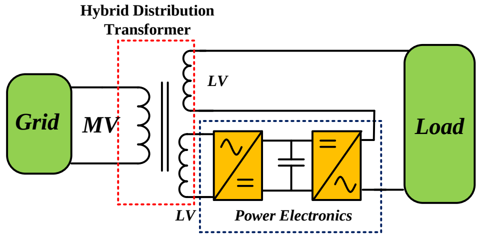

Fig. 3. Configuration of Hybrid Distribution Transformer [22-23].

A similar concept called the hybrid distribution transformer, shown in Fig. 3, has been previously introduced to regulate output voltage by utilizing fractional rated power electronics [22-24]. Also a hybrid transformer utilizing matrix converter was proposed in [25-26]. The concept was proposed in [27] more than a decade ago. However, this system requires a dc-link energy storage system such as the electrolytic capacitor [22-24]. Furthermore, this system requires an additional winding to be wound on the core of the existing bulky line frequency distribution transformer [22-27]. Consequently, this approach adds economical and mechanical constraints for distribution network application because it is required to modify or replace the entire bulky size existing distribution transformer in order to provide voltage compensation functionality in the distribution grid network [28-30].

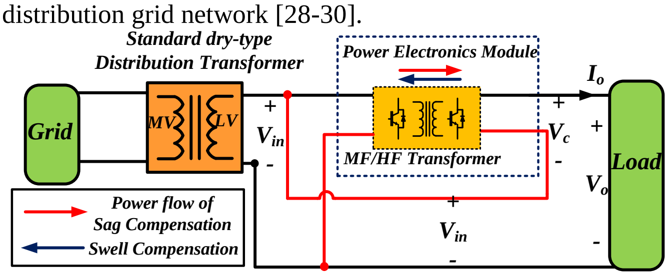

Fig. 4. Conceptual Scheme of the Proposed Distribution Transformer with Power Electronics Module.

This paper introduces a voltage sag and swell compensator that can be easily integrated to the standard dry-type existing distribution transformer without replacing or modifying it. A conceptual schematic of the proposed distribution transformer is shown in Fig. 4. The proposed system is composed of the existing line frequency transformer connected to a power electronics module that is auto-connected on the secondary side in order to compensate for voltage sags and swells. This auto-connection enables shunt-input and series-output compensator without any capacitive energy storage. Hence the proposed system is structurally and functionally different from the conventional series compensator such as *DVR*. The proposed system utilizes the input voltage V_{in} in order to generate the compensating voltage V_c. This is rather considered as a tap changer transformer which regulate the load voltage by varying the turns ratio of the transformer utilizing source voltage instead of using energy storage system in the *DVR*. Due to its structure, the partial power processing capability in the power electronics module allows for a reduced rating in the proposed system. Also, the efficiency can be maximized during the bypass mode in the whole system. The power electronics module generates a compensating voltage, which is vector-added to the grid voltage in order to regulate the output voltage supplied to the load. Moreover, in this paper, the optimized control scheme for the proposed system is introduced in order to achieve dynamic voltage compensation. In terms of power density, the use of a *MF/HF* transformer reduces volume and weight up to 50% and 70% respectively [31], compared to previous approaches which employ an additional line frequency transformer and/or require an additional winding on the existing 50/60Hz core [32-34]. Since the power electronics module is employed without a bulky energy storage system such as electrolytic capacitors, its size and mass can be reduced and the reliability also can be increased [34-35]. The major advantages of the proposed system are:

- The proposed system has a wide range voltage compensation that can correct both the sags and swells of the grid voltage.
- The proposed system can be an easy retro-fit solution, without modifying or replacing the existing distribution transformers.
- The partial power processing capability of the power electronics allows for the reduced power rating of the converter and provides the improved entire efficiency for the system.
- The proposed approach does not need any bulky components such as a *LF* transformer and/or the huge dc-link electrolytic capacitors in the power electronic module, resulting in reduced size and mass.
- Under normal operating conditions, the power electronics module operates in bypass mode, processing no power; it processes power only during disturbance events, resulting in higher reliability and efficiency.
- Under external fault conditions, a bypass switch protects the power electronics module from over current.
- Fast dynamic response is possible.

II. The Proposed System– Concept and Topology

A. *Concept of the Proposed Distribution Transformer*

The proposed system is composed of two parts: a line frequency (*LF*) transformer and a power electronic (*PE*) module as seen in Fig. 4. The *LF* transformer represents a dry-type existing distribution transformer that steps down from medium voltage (*MV*) to low voltage (*LV*) and this provides galvanic isolation between the source voltage and load voltage. The existing *LF* distribution transformer can be retrofitted with the *PE* module, as shown in Fig.4.

One secondary side terminal of the line frequency transformer is connected to an output terminal of the *PE* module so that the load voltage is the sum of the compensating voltage of the *PE* module (V_c) and the secondary side voltage of the standard distribution transformer (V_{in}).

TABLE I THE PROPOSED SERIES VOLTAGE REGULATOR EFFICIENCY CALCULATION

Percentage for amount of voltage disturbance	**Percentage of directly processed power, ρ_m**	**Percentage of partially processed power in power electronics module, ρ_p**	**Calculated overall system efficiency $[\rho_m + (\rho_p \times \eta_c)] \times 100\% = \eta_s$**
50% Swell Case	50%	50%	[0.5+(0.5×0.97)] × 100% = 98.5%
40% Swell Case	60%	40 %	[0.6+(0.4×0.97)] × 100% = 98.8%
20% Swell Case	80%	20%	[0.8+(0.2×0.97)] × 100% = 99.4%
Normal Case	100%	0%	[1+(0×0.97)] × 100% = 100%
20% Swell Case	80%	20%	[0.8+(0.2×0.97)] × 100% = 99.4%
40% Sag Case	60%	40 %	[0.6+(0.4×0.97)] × 100% = 98.8%
50% Sag Case	50%	50%	[0.5+(0.5×0.97)] × 100% = 98.5%

During a voltage sag, (i.e.,$|V_o| > |V_{in}|$), a compensating voltage, V_c from the *PE* module adds to the source voltage (V_{in}), as shown in Fig. 5(a). If a voltage swell occurs, (i.e.,$|V_o| < |V_{in}|$), the *PE* module produces a 180° out-of-phase compensating voltage, as shown in Fig. 5(b). The power flow through the compensation module is reversed during the swell condition. The compensated active power (P_c) from *PE* module is defined as

$$P_c = \left[|V_o|\cdot\cos\theta - |V_{in}|\cdot\cos\theta\right]\cdot|I_o| = |V_c|\cdot\cos\theta\cdot|I_o| \qquad (1)$$

where θ is the load power factor angle.

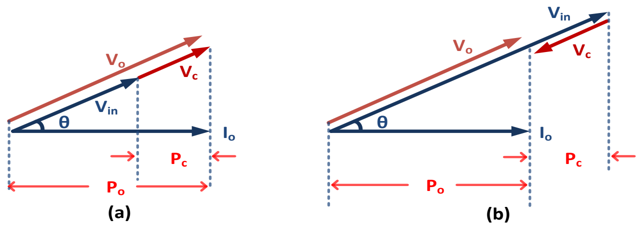

Fig.5.Voltage Vectors for the Compensation of (a) a Voltage Sag and (b) a Voltage Swell.

The efficiency of the proposed system varies based on the amount of bypass power. Thus, the efficiency can be maximized during normal conditions, or bypass mode. Due to fractional power processing of the module, only partial losses of the module is reflected in the entire efficiency calculation of the proposed system. The entire efficiency is calculated as:

$$\eta_s = [\rho_m + (\rho_p \times \eta_c)] \times 100\% \qquad (2)$$

where η_s is the entire efficiency of the proposed system, ρ_m is the percentage of directly processed power, ρ_p is the percentage of the partially processed power in the power electronics module, and η_c is the efficiency of the power electronics module.

With an expected *PE* module efficiency of 97% [31], the entire system's efficiency is calculated with respect to different amounts of voltage sag and swell as shown in Table I.

B. Operating Principal of the Power Electronics Module

The detailed schematic diagram of the *PE* module for the proposed distribution transformer is shown in Fig. 6. The *PE* module consists of four single-phase H-Bridge converters, *MF/HF* transformer, output filter, static bypass switches and *DSP* controller as seen in Fig. 6. Two H-bridge converters (M_2, M_3) connected directly to the *MF/HF* transformer operate at a high switching frequency while the other two converters (M_1, M_4) operate at line frequency. A *MF* transformer can be employed for relatively higher power applications, while a *HF* transformer may be preferred for lower power residential-type applications [34-37].

The *PE* module operates in voltage compensation mode or bypass mode. During bypass mode, the grid-side voltage (V_{in}) is directly connected to the load-side by closing a bypass switch Q_2 and opening a bypass switch Q_1. When voltage sags and swells occur on the grid-side, the bypass switch Q_2 is opened and Q_1 is closed so that the *PWM* switches are activated to supply the required compensating voltage (V_c). Since the bypass switch is activated by a voltage magnitude detection algorithm, the operating bypass mode and compensation mode is determined by voltage magnitude changes in the grid. Moreover, turning on switches S_{3_M4} and S_{4_M4} in the *LF* Unfolding Inverter (M_4) can be utilized in place of having bypass switches Q_1 and Q_2 during normal condition. This reduces switching losses in the entire system by avoiding operating static bypass switches Q_1 and Q_2.

The front-end of the *PE* module, M_1 is a single-phase rectifier hereby addressed a 'low frequency (*LF*) folding converter. The *LF* folding converter operates at line frequency (50 / 60Hz) (see Fig. 7(b)), generating pulsating dc from the ac source as shown in Fig. 7(c).

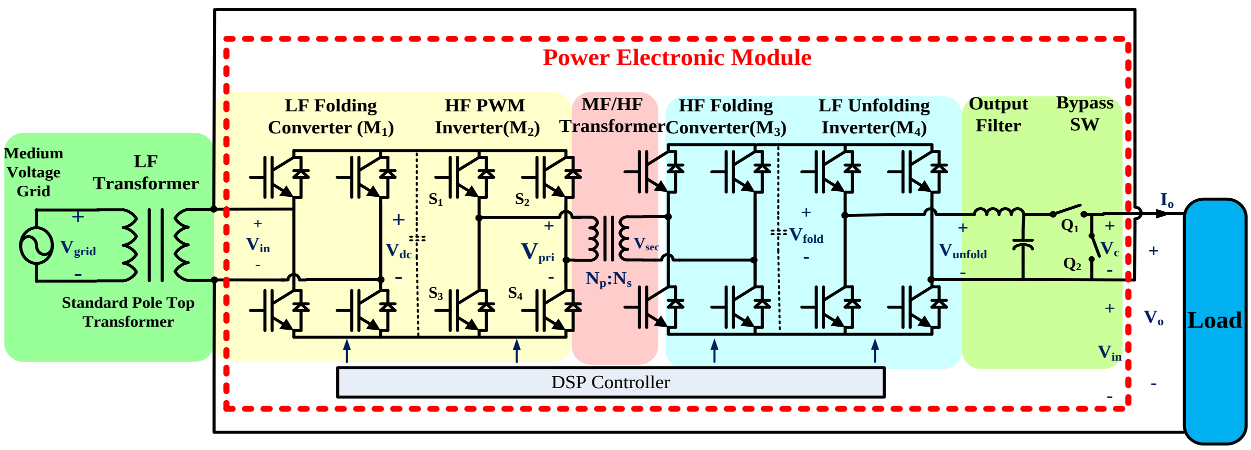

Fig. 6. Detailed Power Electronics Module in the Proposed Distribution Transformer.

This article has been accepted for publication in a future issue of this journal, but has not been fully edited. Content may change prior to final publication. Citation information: DOI 10.1109/TIE.2017.2668982, IEEE Transactions on Industrial Electronics

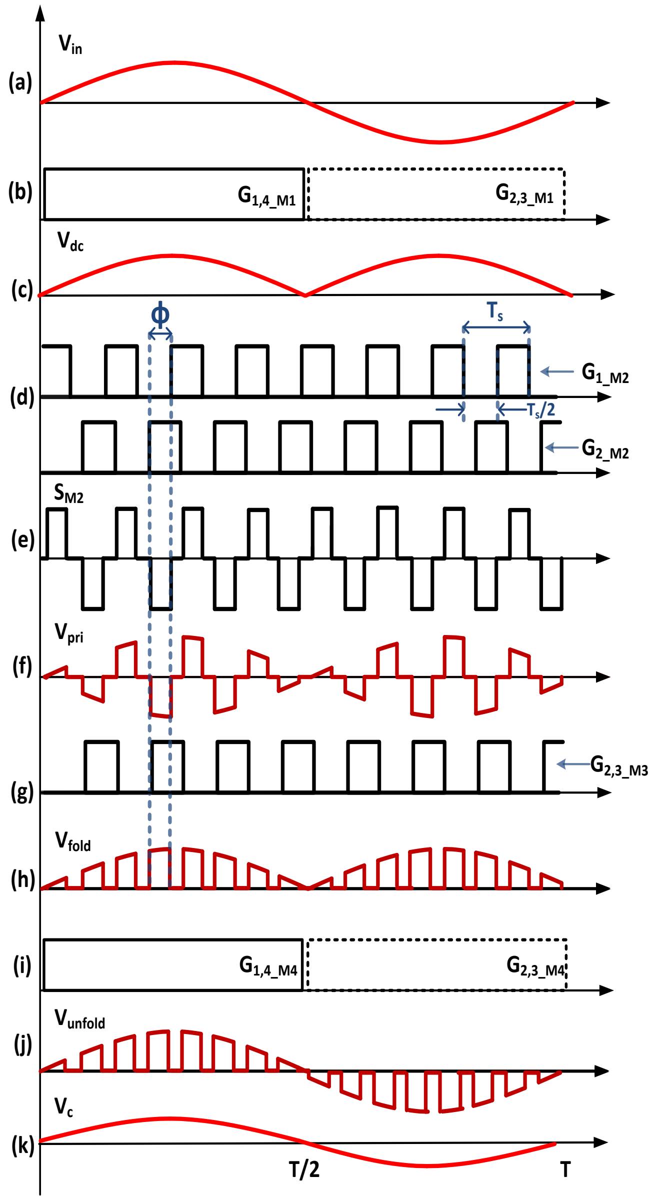

Fig. 7. Operating Waveforms of *PE* Module for Sag Operation: (a) source voltage, V_{in}. (b) M_1 gate signal, G_{m1}. (c) *LF* rectified voltage, V_{dc}. (d) M_2 gate signal, G_{m2}. (e) switching function of M_2, s_{m2}. (f) primary voltage of *MF/HF* transfomrer, V_{pri}. (g) M_3 gate signal, G_{m3}. (h) *LF* folded voltage, V_{fold}. (i) M_1 gate signal, G_{m1}. (j) *lf* unfolded voltage, V_{unfold}. (k) compensating voltage, V_c.

The pulsating double line frequency voltage ripple can be expressed as

$$V_{dc} = \sqrt{2} \cdot V_{rms} \left(\frac{2}{\pi} - \frac{4}{\pi} \sum_{n=2,4,6...}^{\infty} \frac{\cos(n\omega_o t)}{n^2 - 1} \right) \tag{3}$$

A *MF/HF* voltage is generated from the pulsating dc voltage by the *HF PWM* inverter (M_2) using the phase-shifted modulation technique. The phase shift angle, ϕ is adjusted in order to regulate load voltage as shown in Fig. 7(d). The switching function S_{M2} for the converter M_2 is shown in Fig. 7(e) and can be described as

$$S_{M2} = \frac{4}{\pi} \cdot \sum_{n=1,3,5...}^{\infty} \frac{1}{n} \cdot \sin\left(n\omega_s t + \frac{\pi - n\phi}{2}\right) \cdot \sin\left(\frac{n\phi}{2}\right) \tag{4}$$

Therefore, the primary voltage of the *MF/HF* transformer is shown in Fig. 7(f) and is given as

$$V_{pri} = V_{dc} \cdot S_{M2}$$
$$= \left(1.62 \cdot \sqrt{2} \cdot V_{rms}\right) \cdot \begin{bmatrix} \sin\left(\omega_s t + \frac{\pi - \phi}{2}\right) \cdot \sin\left(\frac{\phi}{2}\right) \\ -\frac{1}{3} \sin\left(3\omega_s t + \frac{\pi - 3\phi}{2}\right) \cdot \sin\left(\frac{3\phi}{2}\right) \\ +\frac{1}{3\pi} \sin\left\{(\omega_s \pm 2\omega_o)t + \frac{\pi - \phi}{2}\right\} \cdot \sin\left(\frac{\phi}{2}\right) \\ \cdots \\ + \textit{higher order terms} \end{bmatrix} \tag{5}$$

Note that V_{pri} has no low frequency components such as line frequency or its harmonic components, and the major frequency component of the *MF/HF* transformer are odd multiples of the switching frequency ω_s and their sideband components $\omega_s \pm 2\omega_o$ as seen in (5).

The sada Fig. 7(j). During a swell condition, the unfolded output voltage of M_4 becomes a 180° out-of-phase with respect to the input voltage. Afterward, a small output filter attenuates the *HF* components in the compensating voltage, V_c as seen in Fig. 7(k).

C. MF/HF Transformer Turns Ratio and VA Rating

The compensating voltage, V_c is regulated to be the difference between grid-side voltage V_{in} and the desired load voltage ($V_{o,ref}$), as seen in (6).

$$V_c = V_{o,ref} - V_{in} \tag{6}$$

Set the required compensating voltage, V_c to be

$$V_c = -k \cdot V_{o,ref} \tag{7}$$

where "*k*" represents the amount of voltage sag/swell magnitude per unit ($k < 0$ for sag and $k > 0$ for swell), e.g. $V_c = -0.2V_o$ for a 20% voltage swell case, and $V_c = 0.3V_c$ for *a* 30% voltage sag case.

Then, the grid-side voltage V_{in} can be expressed from (6) and (7) by

$$V_{in} = (1 + k) \cdot V_{o,ref} \tag{8}$$

From Fig. 5, the output of *PE* module V_c, the required compensating voltage, is described as

$$V_c = V_{in} \cdot \frac{\phi}{\pi} \cdot \frac{N_p}{N_s} \tag{9}$$

where $\phi \in [0, \ \pi]$

Hence, the compensated load side voltage, $V_{o,ref}$ can be expressed as

$$V_{o,ref} = (1 + k) \cdot V_{o,ref} + \frac{\phi}{\pi} \cdot (1 + k) \cdot V_{o,ref} \cdot \frac{N_p}{N_s} \tag{10}$$

Consequently, the relationship between the *MF/HF* transformer turns ratio $N_p{:}N_s$ and the range of the compensation voltage sag/swell becomes

$$\frac{N_p}{N_s} = \frac{\pi}{\phi} \cdot \left| \frac{k}{1 + k} \right| \tag{11}$$

From (11) the range of the compensation for the sag/swell relative to the phase angle ϕ can be obtained as shown in Fig. 8. It is seen that voltage sags up to 50% of grid voltage could be compensated when $N_p{:}N_s$ ratio is 1:1. The variation of the phase

This article has been accepted for publication in a future issue of this journal, but has not been fully edited. Content may change prior to final publication. Citation information: DOI 10.1109/TIE.2017.2668982, IEEE Transactions on Industrial Electronics

shift angle ϕ for the sag compensation is wider than that of the swell compensation as seen in Fig. 8. In terms of the system stability, the compensation threshold limit can be also determined by the amount of feeder impedance.

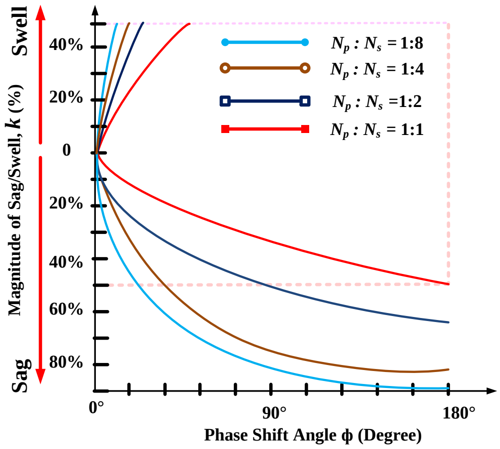

Fig. 8. Phase Shifting Angle Variation as Turns Ratios Changes in the *PE* Module.

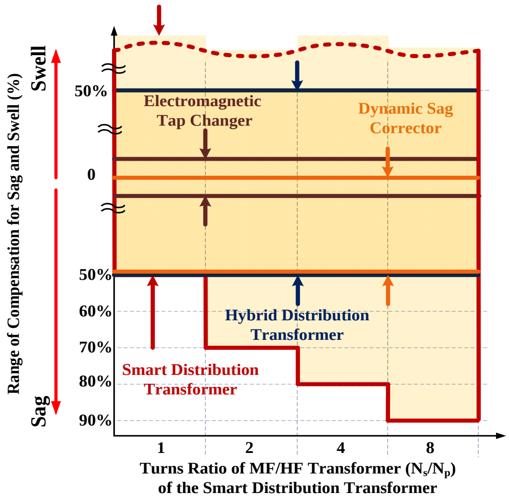

Fig.9. Comparison for Range of Compensation for Voltage Sag/Swell.

Fig. 9 shows a comparison of the range of voltage compensation for three different types of distribution transformer – electromagnetic tap changer, dynamic sag corrector, hybrid distribution transformer [8-26] and the proposed distribution transformer. It is noted that a wide range of compensation can be achieved by optimizing the turns ratio of *MF/HF* transformer in the proposed system. As seen from Figs. 8 and 9, as the number of turns in the *MF/HF* transformer secondary increases, it becomes possible to compensate for deeper sag and swell events.

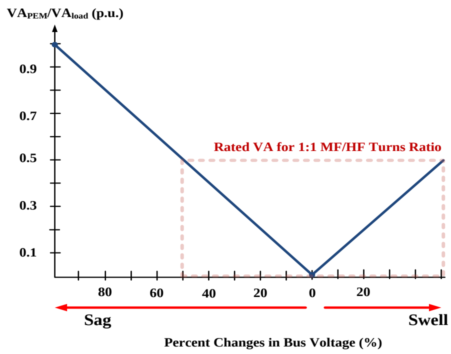

Fig. 10. VA ratio *MF/HF* transformer to load.

The ratio of *MF/HF* transformer *VA* to load *VA* with no feeder impedance is shown in Fig. 10. The *VA* ratio increases as amount of sag or swell increases. In other words, only partial power is processed in the *MF/HF* transformer to compensate for that amount of the voltage sag or swell. Therefore, *VA* rating of *MF/HF* transformer, which is also the *VA* rating of the *PE* module, can be determined based on the magnitude of the voltage disturbance. Also, *PE* module *VA* rating can be slightly effected by the resistance or inductance of the source if the feeder impedance are significant.

D. Closed Loop Control Strategy

The control scheme for the proposed system is introduced in this section. Fig. 11 shows operation waveform of the proposed control scheme based on the control block diagram in Fig. 12. The control block diagram includes a load voltage control block and a compensating voltage reference generation block as seen in Fig. 12. When the voltage sag/swell occurs, the compensating voltage reference generation block generates duty ratio D_{ff}, based on the amount of voltage sag/swell. Also, the load voltage control block generates duty ratio D_{fb}, to regulate the desired load voltage.

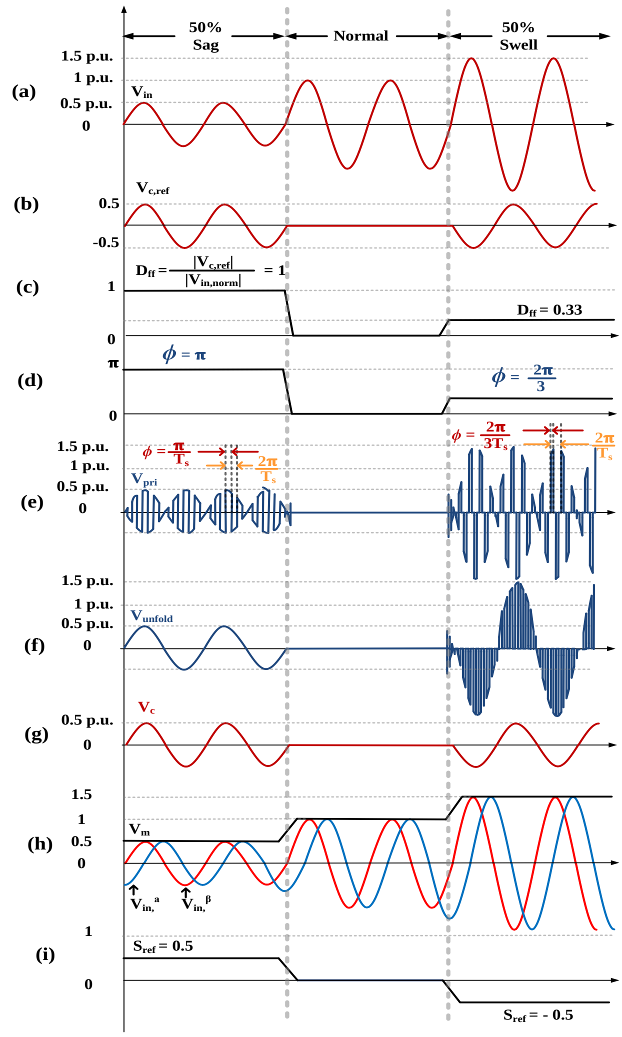

Fig. 11. Ideal Operation for Phase Shift Modulation in the Proposed Control Scheme at 1:1 Turns Ratio: (a) source voltage v_{in} with 50% sag, normal and 50% swell, (b) compensating reference signal $v_{c,ref}$, (c) duty, D_{ff}, (d) phase shift angle ϕ, (e) primary voltage of *MF/HF* transformer, v_{pri}, (f) unfolded voltage, V_{unfold}, (g) compensating voltage V_c, (h) normalized source voltage V_{in}^{β}, 90° phase delay normalized source voltage V_{in}^{α}, and normalized input voltage magnitude V_m, and (i) voltage detection signal, S_{ref} .

This article has been accepted for publication in a future issue of this journal, but has not been fully edited. Content may change prior to final publication. Citation information: DOI 10.1109/TIE.2017.2668982, IEEE Transactions on Industrial Electronics

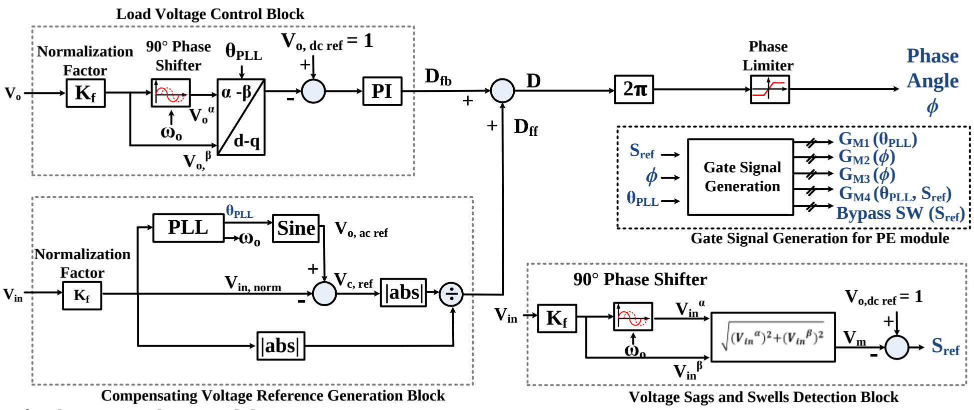

Fig. 12. Control Scheme for the Proposed *PE* Module.

The compensating voltage reference, $V_{c,\,ref}$, shown in Fig. 11 (b) for voltage sag or swell is obtained by subtracting the normalized grid voltage signal, $V_{in,norm}$, from the normalized ac reference signal, $V_{o,ac\;ref}$, the unity magnitude sinusoidal signal generated by the fundamental frequency detection methods [38-39]. The calculated duty ratio D_{ff} from feedforward loop shown in Fig. 11(c) can be expressed as

$$D_{ff} = \frac{\left|V_{o,ac\_ref} - V_{in,norm}\right|}{V_{in,norm}} = \frac{\left|V_{c,ref}\right|}{\left|V_{in,norm}\right|} \qquad (12)$$

The angle of phase delay (ϕ) in the control scheme is obtained by a conversion of the duty ratio radian after adding D_{ff} and D_{fb} as seen in Fig. 11(d). Then, this phase angle delay ϕ, is adjusted in order to generate compensating voltage V_c as shown in Figs. 11 (e), (f) and (g).

In the compensating voltage sags and swells detection block, a voltage magnitude of the input voltage, V_m is obtained as shown in Fig. 11 (h) and is expressed as

$$V_m = \sqrt{(V_{in}^{\alpha})^2 + (V_{in}^{\beta})^2} \qquad (13)$$

where V_{in}^{β} is a normalized input voltage and V_{in}^{α} is a 90° phase shifted normalized input voltage

A voltage detection signal S_{ref} for voltage sag or swell is determined by subtracting V_m signal from normalized dc reference voltage signal $V_{o,\,dc\;ref}$ as shown in Fig. 11 (i). These are described as

$$S_{ref} = \begin{cases} 0 & (\text{no sag or swell}) \\ > 0 & (\text{sag case}) \\ < 0 & (\text{swell case}) \end{cases} \qquad (14)$$

It is noted that the gate signals of each converter in the *PE* module, and bypass switch in the *PE* module are generated by implementing the zero crossing angle θ_{PLL}, the phase shift angle ϕ and the voltage detection signal S_{ref} as seen in Fig. 12.

As shown in Fig. 11 (e), the primary voltage, V_{pri} is generated *HF* based on the obtained phase shift angle ϕ from the control scheme. Assuming that a 1:1 *MF/HF* transformer is selected, the compensating voltage for 50% sag condition can be generated by superimposing the maximum phase angle ϕ which is **π** in rad on the 50% sagged line frequency pulsating voltage as shown in Figs. 11 (e), (f) and (g). For the 50% swell condition, the primary voltage has $\frac{2\pi}{3}$ in rad phase delay superimposed on a line frequency swelled pulsating voltage as shown in Fig. 11 (e). The 180° out-of-phase compensating voltage V_c is provided by filtering out *HF* components from unfolded voltage as shown in Fig. 11 (f) and (g).

III. Experimental Test Setup and Results

A scaled-down 1.2 kW laboratory prototype for the proposed system with 120 V_{rms} / 60Hz source voltage was constructed and tested as shown in Fig. 13. The operating condition, devices rating and *MF/HF* transformer design parameters are shown in Table II, and III. The controller was implemented with the Texas Instruments *TMS320F28335* controller and the power devices used were Semikron *IGBT* modules.

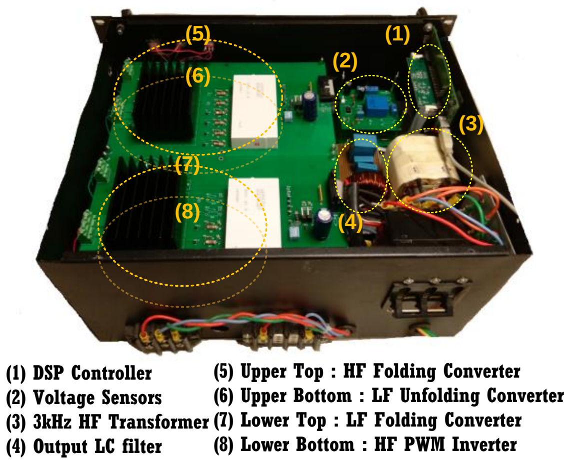

Fig. 13. Prototype of the Power Electronics Module.

Table II Summary of Parameter for HF Transformer

Phase Type	Single Phase
Core Material	Si-Steel
Operating Switching Frequency, f_s (Hz)	3000
Turns Ratio	1:1
Peak Flux Density, B_{peak} (Tesla)	2.0
Input / Output Voltage RMS (V)	80/80
Rated VA	850
Number of Turns in Primary Side	7 (3)
Number of Turns in Secondary Side	7 (3)

Table III Component Ratings of the PE Module

Devices	Rating
IGBT Devices (S_1-S to Q_1-Q_4 of *HF* converters and switches of *LF* converters)	250V (1.5 p.u.) 12 A_{rms} (1 p.u.)
Output Filter Inductor L_f = (4 mH)	12 A_{rms} (1 p.u.)
Output Filter Capacitor C_f = (7.5μF)	85V (0.5 p.u.)
Small coupling capacitor C_{dc} = (0.8μF)	250 V (1.5 p.u.)

The converter ratings are selected based on the maximum change in voltage during sag/swell condition. The cut-off frequency of the filter is a 950Hz and the size of the output filter

This article has been accepted for publication in a future issue of this journal, but has not been fully edited. Content may change prior to final publication. Citation information: DOI 10.1109/TIE.2017.2668982, IEEE Transactions on Industrial Electronics

is determined by the operating frequency of HF transformer. In other words, smaller output filter can be selected if the operating frequency of the HF transformer is increased. In this experiment, two *IGBTs* S_{3_M4} and S_{4_M4} in the unfolding converter (M_4) were utilized as bypass switches instead of adding mechanical switches Q_1 and Q_2 in Fig. 6.

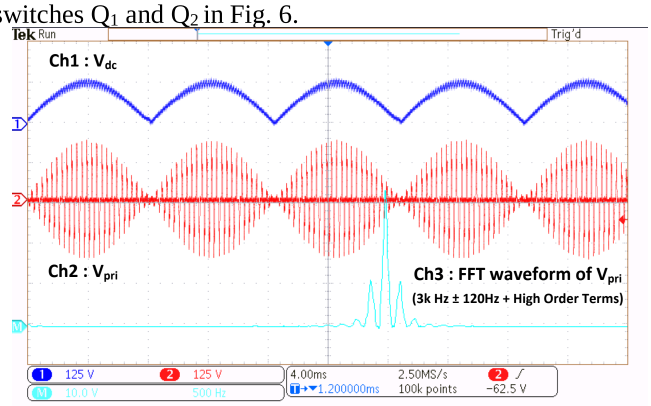

Fig. 14. Ch1: LF Rectified Voltage, V_{dc}, Ch2: Primary Voltage of Transformer, V_{pri} and Ch3: Frequency Spectrum.

Fig. 14 shows the primary voltage of the *HF* transformer. The *HF* quasi-pulsating dc voltage V_{pri} can be seen in Ch2 and the frequency spectrum of Ch3 shows a 3 kHz switching frequency along with ±120 Hz components as derived in (5).

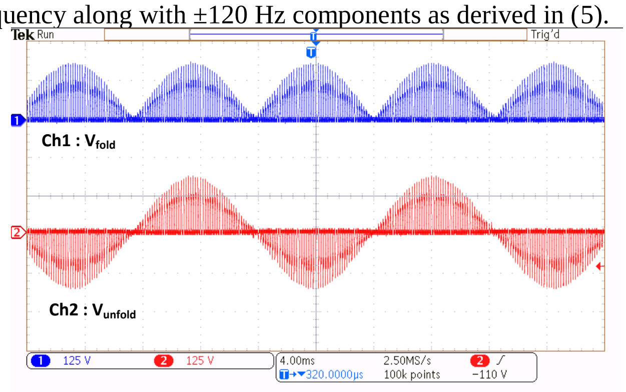

Fig. 15. Ch1 : Folded Voltage, V_{fold} and Ch2 : Unfolded Voltage, V_{unfold}.

In Fig. 15, folded voltage including *HF* components (V_{fold}) can be seen in Ch1. By 60 Hz unfolding switching operation, the *HF* fixed duty chopped 60 Hz sinusoidal voltage (V_{unfold}) is obtained, shown in Ch2. This unfolded voltage becomes the compensator output voltage V_c after *HF* components are filtered out, to generate the nominal voltage 120V.

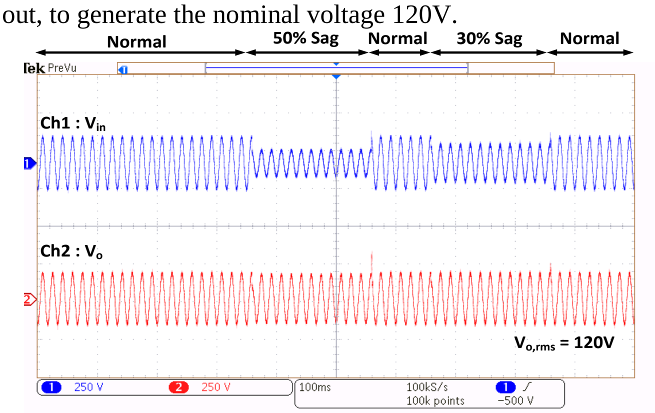

Fig. 16. Ch1 : Source Voltage With 50% Sag and 30% Sag Respectively, V_{in} Ch2 : Compensated Load Voltage V_o.

The dynamic compensating operation of the proposed system with resistive load is shown in Figs 16, 17 and 18 in various conditions. Figs. 16, 17 and 18 shows that the load voltage V_o is well regulated with a nominal 120V under a resistive load by the proposed system. The corresponding voltage waveforms when the input voltage has 50% and 30% sags are shown in Fig. 16. Fig. 17 shows that consequent 9 cycles of 25% and 38% voltage swell conditions respectively are compensated in the 120V nominal load voltage. Fig. 18 shows the dynamic response of compensation for both of sag and swell conditions. Fig. 19 shows the input voltage transient response for a 45% voltage sag condition. Due to the digital filter and the control algorithm computation time for detecting sags, a small delay exists. It is observed that the transient response time is 3.2 ms, which is less than 1/4 cycle (4.1 ms) in the experiment, while converting to the compensation mode from the bypass mode.

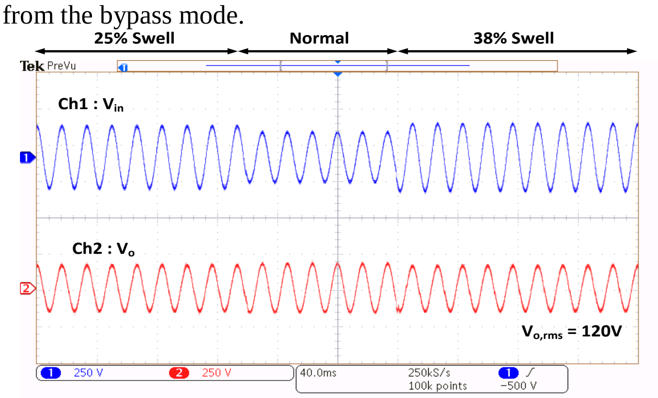

Fig. 17. Ch1 : Source Voltage with 25% Swell and 38% Swell Respectively, V_{in} Ch2 : Compensated Load Voltage V_o.

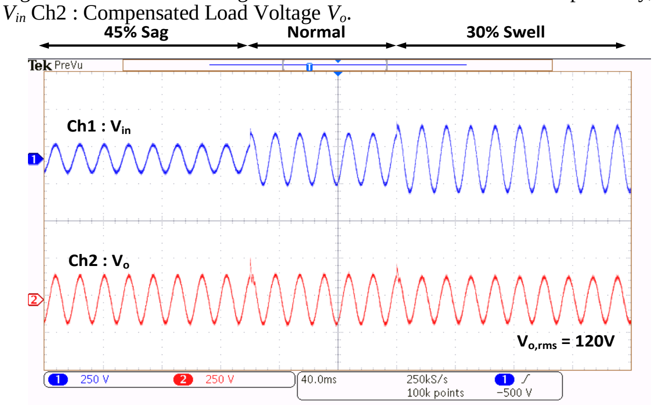

Fig. 18. Ch1 : Source Voltage with 40% Sag and 25% Swell Respectively, V_{in} Ch2 : Compensated Load Voltage, V_o.

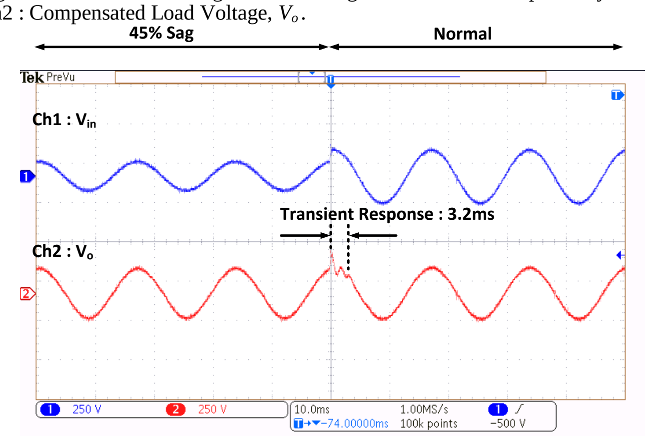

Fig. 19. Voltage Transient Responses for 45% Sag Condition, Ch1: Source Voltage, Ch2: Load Voltage, V_o.

The experimental results with the rectifier load are shown in Fig. 20. The compensator can operate under the 35% voltage sag with nonlinear load as shown in Ch1 and Ch2. During the bypass mode with nominal voltage, the current of *HF* transformer primary side, I_{pri} is zero which means no power is processed by the power electronics module as shown in Ch.4. It

This article has been accepted for publication in a future issue of this journal, but has not been fully edited. Content may change prior to final publication. Citation information: DOI 10.1109/TIE.2017.2668982, IEEE Transactions on Industrial Electronics

is noted that load voltage V_o is somewhat distorted since the inductor size of the output filter is relatively big according to its cut-off frequency. This can be improved by decreasing the inductance value in the filter and/or the increase of the operating frequency of *HF* transformer with its higher cut-off frequency.

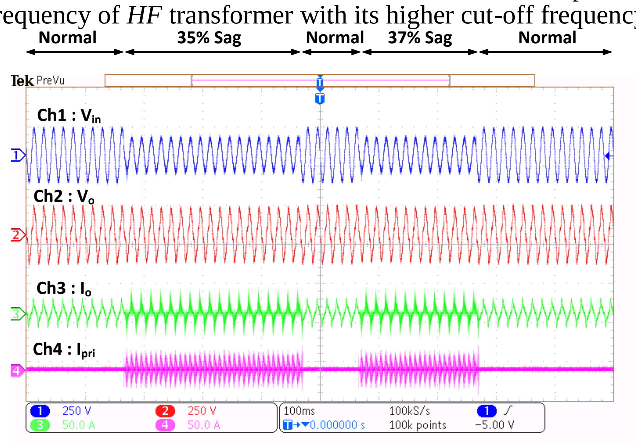

Fig. 20 Ch1 : Source Voltage with 45% Sag with Nonlinear Load V_{in} Ch2 : Compensated Pure Nonlinear Load Voltage *Vo* Ch3 : Nonlinear Load Current I_o Ch4 : Current Of *HF* Transformer Primary Side, I_{pri}.

IV. Conclusion

In this paper, a series voltage regulator for the distribution transformer to compensate voltage sags/swells along with its control scheme has been introduced. The proposed approach can be easily integrated into existing conventional distribution transformers in order to provide sag or swell compensation capability for a distribution grid system. Experimental results demonstrate voltage sag and swell compensation without a dc-link and associated electrolytic capacitors. Due to partial power processing, the *PE* module has a lower voltage rating and, for the same reason, the *MF/HF* transformer has a lower *VA* rating than the load. Therefore, the proposed system is a possible retro-fit solution for existing distribution transformers to improve power quality in the future grid**,** especially in the face of the proliferation of renewable and distributed generation**.**

References

[1] T. Strasser et al., "A review of architectures and concepts for intelligence in future electric energy systems," *IEEE Trans. Ind. Electron*., vol. 62, no. 4, pp. 2424–2438, Apr. 2015.

[2] M.J. Sullivan, T. Vardell, and M. Johnson, "Power interruption costs to industrial and commercial consumers of electricity," in *IEEE Industrial and Commercial Power Systems Technical Conf. Rec*., pp. 23-35, 1996.

[3] McGranaghan M, Roettger B. "Economic evaluation of power quality," *IEEE Power Engineering Review*, vol. 22(2), pp 8–12, 2002.

[4] Moreno-Muñoz, A.; Flores-Arias, J.M.; Pallarés, V.; De la Rosa, and J.J.G. "Power quality immunity in factory automation," *Compatibility and Power Electronics*, CPE '09, pp 12 – 17, 2009.

[5] S. Bhattacharyya, J. M. A. Myrzik, and W. L. Kling, "Consequences of poor power quality: An overview," in *Proc. 42nd Int. Univ. Power Eng. Conf.*, pp. 651–656, 2007.

[6] Shih-An Yin, Chan-Nan Lu, Edwin Liu, et al. "A survey on high- tech industry power quality requirements," *IEEE/PES Transmission and Distribution Conference and Exposition.* Vol. 1, pp 548–553, 2001.

[7] Recommended Practice for Monitoring Electric Power Quality, *IEEE 1159/2009*, 2009.

[8] Brumsickle, W.E.; Schneider, R.S.; Luckjiff, G.A.; Divan, D.M.; Mc Granaghan, M.F.; "Dynamic sag correctors: cost-effective industrial power line conditioning," *IEEE Transactions on Industry Applications*, vol: 37, No. 1, pp: 212 –217, Feb. 2001.

[9] J. Kyei, R. Ayyanar, G. T. Heydt, R. Thallam, J. Blevins, "The design of power acceptability curves," *IEEE Trans Power Deliv.*, vol.17 pp. 828–833, Nov. 2002.

[10] D. Gao, Q. Lu, and J. Luo, "A new scheme for on-load tap-changer of transformers," in *Proc. Int. Conf. Power System Technology*, pp. 1016–1020, 2002.

[11] N. Yorino, M. Danyoshi and M. Kitagawa, "Interaction Among Multiple Controls in Tap Change Under Load Transformers," *IEEE Transactions on Power System*, vol. 12, no. 1, pp. 430434, Feb. 1997.

[12] M.S. Calovic, "Modeling and analysis of under-load tap changing transformer control systems," *IEEE Transactions on Power Apparatus and Systems*, Vol. 103, pp. 1909-1915, Jul. 1984.

[13] A. Prasai and D. M. Divan, "Zero-energy sag correctors—Optimizing dynamic voltage restorers for industrial applications," *IEEE Trans. Ind. Appl.*, vol. 44, no. 6, pp. 1777–1784, Nov./Dec. 2008.

[14] O. C. Montero-Hernandez and P. N. Enjeti, "Application of a boost AC-AC converter to compensate for voltage sags in electric power distribution systems," in *Proc. Power Electronics Specialists Conference, PESC,* vol. 1, pp. 470–475 , 2000.

[15] O.C. Montero-Hernandez and P.N. Enjeti, "Ride-Through for Critical Load. Exploring a Low-Cost Approach to Maintaining Continuous Connections Between Buildings and/or Industrial Systems," *IEEE Ind. Appl. Mag.*, vol.8, pp.45-53, Nov-Dec 2002.

[16] E. C. Aeloíza, P. N. Enjeti, L. A. Morán, O. C. Montero Hernandez, and S. Kim, "Analysis and design of a new voltage sag compensator for critical loads in electrical power distribution systems," *IEEE Trans. Ind. Appl*.,vol. 39, no. 4, pp. 1143–1150, Jul./Aug. 2003.

[17] A. K. Sadigh and K. M. Smedley, "Review of voltage compensation methods in dynamic voltage restorer (DVR)," in *Proc. IEEE Power Energy Soc. Gen. Meet.*, pp. 1–8, Jul. 2012.

[18] S. S. Choi, J. D. Li, and D. M. Vilathgamuwa, "A generalized voltage compensation strategy for mitigating the impacts of voltage sags/swells," *IEEE Trans. Power Delivery*, vol. 20, no. 4, pp. 2289–2297, Jul. 2005.

[19] A. Rauf and V. Khadkikar, "An enhanced voltage sag compensation scheme for dynamic voltage restorer," *Industrial Electronics, IEEE Transactions on*, vol. 62, pp. 2683–2692, May 2015.

[20] S. Lee., H. Cha, and B. Han, "A new single-phase voltage sag/swell compensator using direct power conversion," in *Proc. Energy Conversion Congress and Exposition*, pp 2704 – 2710, 2009.

[21] S. Jothibasu and M. K. Mishra, "An improved direct AC–AC converter for voltage sag mitigation," *IEEE Trans. Ind. Electron*., vol. 62, no. 1, pp. 21–29, Jan. 2015.

[22] S. Bala, D. Das, E. Aeloiza, A. Maitra, and S. Rajagopalan, "Hybrid distribution transformer: Concept development and field demonstration," in *Proc. IEEE Energy Convers. Congr. Expo*, pp. 4061– 4068, 2012.

[23] Sastry, J., Bala, S. "Considerations for the design of power electronic modules for hybrid distribution transformers," *Energy Conversion Congress and Exposition (ECCE), IEEE,* On page(s): 1422 – 1428, 2013.

[24] Radi, M.A., Darwish, M.; Alqarni, M. "Voltage regulation considerations for the design of hybrid distribution transformers," *Power Engineering Conference (UPEC), 49th International Universities,* On page(s): 1–6, 2014.

[25] J. Kaniewski, Z. Fedyczak, and G. Benysek, "AC voltage sag/swell compensator based on three-phase hybrid transformer with buck-boost matrix-reactance chopper," *IEEE Trans. Ind. Electron.*, vol. 61, no. 8, pp. 3835–3846, Aug. 2014.

[26] J. Kaniewski, P. Szczesniak, M. Jarnut, and G. Benysek, "Hybrid Voltage Sag/Swell Compensators: A Review of Hybrid AC/AC converters," *IEEE. Industrial Electronics. Magazine*, vol. 9, pp. 37–48, 2015.

[27] E. Aeloiza, P. Enjeti, L. Moran, and I. Pitel, "Next generation distribution transformer: to address power quality for critical loads," in *IEEE Power Electronics Specialist Conference (PESC)*, vol. 3, June 2003.

[28] P. Balducci, L. Schienbein, T. Nguyen, D. Brown, and E. Fathelrahman, "An examination of the costs and critical characteristics of electric utility distribution system capacity enhancement projects," in *Proc. IEEE Transmission and Distribution Conf. and Expo.*, Dallas, TX, USA, pp. 78–86, 2006.

[29] P.R. Barnes, J.W. Van Dyke, B.W. McConnell, S.M. Cohn, S.L. Purucker, "The Feasibility of replacing or upgrading utility distribution transformers during routine maintenance," *Power Systems Technology program, Oak Ridge National Lab*, Tennessee, USA, Final Rep. DOE AC05840R2140000, April, 1995.

[30] 'Transformer Retrofit considerations,' [Online] Available : < http://criticalpowergroup.com/wp-content/uploads/Transformer-Retrofit-Considerations-002603-007-A03.pdf>.

[31] M. K. Das, C. Capell, D. E. Grider, R. Raju, M. Schutten, 1. Nasadoski, S. Leslie, J. Ostop, A. Hefner; "10 kV, 120 A SiC Half H-Bridge Power MOSFET Modules Suitable for High Frequency, Medium Voltage Applications," *IEEE, ECCE*, pp.2689–2692, 2011.

[32] G. Ortiz, J. Biela, and J. W. Kolar, "Optimized design of medium frequency transformers with high isolation requirements," in *Proc. IEEE Ind. Electron*, pp. 631–638, Sep., 2010

[33] X. She, A. Huang, and R. Burgos, "Review of solid-state transformer technologies and their application in power distribution systems," *IEEE J. Emerging Sel. Topics Power Electron*., vol. 1, no. 3, pp. 186–198, Sep. 2013.

[34] H. S. Krishnamoorthy, D. Rana, P. Garg, P. N. Enjeti, and I. J. Pitel, "Wind turbine generator-battery energy storage utility interface converter topology with medium-frequency transformer link," *IEEE Trans. Power Electron*., vol. 29, no. 8, pp. 4146–4155, Aug. 2014.

[35] H. S. Krishnamoorthy, P. Garg, and P. N. Enjeti, "A matrix converter-based topology for high power electric vehicle battery charging and V2G application," in *38th Annual Conference on IEEE Industrial Electronics Society*, pp. 2866-2871, 2012.

[36] Y. Zhuang, C. Wang, C. Wang, H. Cheng, Y. Gong, H. Wang, "Determination Method for Topology Configuration of Hybrid Cascaded H-Bridge Rectifiers," *J. Power Electron.*, vol. 16, no. 5, pp. 1763-1772, Sept. 2016.

[37] J. Shang, X. Nian, T. Chen, Z. Ma, "Grid-friendly Control Strategy with Dual Primary-Side Series-Connected Winding Transformers," *J. Power Electron.*, vol. 16, no. 3, pp. 960-969, May 2016.

[38] L. Asiminoaei, F. Blaabjerg, S. Hansen "Detection is key - harmonic detection methods for active power filter applications," *IEEE Industry Applications Magazine* 13(4), pp. 22-33, 2007

[39] Morsy, A.S.; Enjeti, P.; Ahmed, S.; Massoud, A., "Phase locked loop with fast tracking over wide stability range under grid faults," in *Applied Power Electronics Conference and Exposition (APEC), 2014 Twenty-Ninth Annual IEEE* , vol., no., pp.1263-1267, 16-20 March 2014

Taeyong Kang (S'14) received the B.Sc degree in electrical engineering from the Kyungpook National University, Daegu, South Korea, in 2013 and the M.S. degree in electrical engineering from the Texas A&M University, College Station, TX, USA in 2016.

He is currently an electrical engineer at the OTIS Elevator Company R&D center - United Technologies Corporation, Farmington, CT, USA. During his graduate study, he was a Power Electronics Intern with Schlumberger Technology Corporation Research and Engineering Group, Sugar Land, TX, USA and Electrical Engineer Intern with United Technologies Corporation, Farmington, CT, USA, where he is currently working for. His research interests include mainly power electronics applications in motor drive and power quality.

Sewan Choi (S'92-M'96-SM'04) received the B.S. degree in electronic engineering from Inha University, Incheon, Korea, in 1985 and the M.S. and Ph.D. degrees in electrical engineering from Texas A&M University, College Station, TX, in 1992 and 1995, respectively. From 1985 to 1990, he was with Daewoo Heavy Industries as a Research Engineer. From 1996 to 1997, he was a Principal Research Engineer at Samsung Electro-Mechanics Co., Korea. In 1997, he joined the Department of Electrical and Information Engineering, Seoul National University of Science and Technology(Seoul Tech), Seoul, Korea, where he is currently a Professor. His research interests include power conversion technologies for renewable energy systems and energy storage systems and DC-DC converters and battery chargers for electric vehicles. He is an Associate Editor of the IEEE TRANSACTIONS ON POWER ELECTRONICS and IEEE JOURNAL OF EMERGING AND SLECTED TOPICS IN POWER ELECTRONICS.

Ahmed S. Morsy (M'10) received the B.Sc and M.Sc. degrees from Alexandria University, Alexandria, Egypt, in 2008 and 2011, respectively, and the Ph.D. degree from Texas A&M University, College Station, in 2016, all in electrical engineering.

He is currently an Electrical Engineer with Schlumberger Technology Corporation Research and Engineering Group, Sugar Land, TX, USA. During his Ph.D. degree, he was a Graduate Intern with Dell Inc. advanced power group, Round Rock, TX, USA, and ABB corporate research center, Raleigh, NC, USA. From 2008 to 2012, he was a teaching assistant with the Electrical Engineering Department, Faculty of Engineering, Alexandria University. From 2008 to 2011, he was with Spiretronic LLC as a Research Engineer where he invented a new topology to increase energy harvesting from PV farms. He holds one US patent in addition to several IEEE journal/conference papers. His research interests are power electronics control, high frequency, high density design using wide band gap devices, utility interface and power quality, power conditioning for wind and solar energy systems, Multilevel Converters, and sensorless control and fault tolerant operation of multi-phase machines.

Prasad N. Enjeti (M'85–SM'88–F'00) received the B.E. degree from Osmania University, Hyderabad, India, in 1980, the M.Tech. degree from IIT Kanpur, Kanpur, India, in 1982, and the Ph.D. degree from Concordia University, Montréal, QC, Canada, in 1988, all in electrical engineering. He joined the Department of Electrical Engineering, Texas A&M University, College Station, TX, USA, as an Assistant Professor, in 1988. He was promoted to an Associate Professor in 1994, and he became a Full Professor in 1998. He holds four U.S. patents and has licensed two new technologies to the industry so far. He is currently the lead Developer of the Power Electronics/Power Quality and Fuel Cell Power Conditioning Laboratories, Texas A&M University, and is actively involved in many projects with industries while engaged in teaching, research, and consulting in the area of power electronics, motor drives, power quality, and clean power utility interface issues. His current research interests include advance converters for power supplies and motor drives, power quality issues and active power filter development, converters for fuel cells, wind energy systems, power electronic hardware for flywheel, ultracapacitor type energy storage/discharge devices for ride-through, and utility interface issues. Dr. Enjeti received the inaugural R. David Middlebrook Technical Achievement Award from the IEEE Power Electronics Society in 2012. He received the IEEE-IAS Second and Third Best Paper Awards in 1993, 1996, 1998, 1999, and 2001, the Second Best IEEE-IA TRANSACTIONS paper published from 1994 to 1995, the IEEE-IAS Magazine Prize Article Award in 1996, the Class of 2001 Texas A&M University Faculty Fellow Award for the demonstrated achievement of excellence in research, scholarship, and leadership in the field, and he directed a team of students to design and build a low cost fuel cell inverter for residential applications, which won the 2001 Future Energy Challenge Award, grand prize, from the Department of Energy. He is a registered Professional Engineer in the state of Texas.